Since January 2020 Elsevier has created a COVID-19 resource centre with free information in English and Mandarin on the novel coronavirus COVID-19. The COVID-19 resource centre is hosted on Elsevier Connect, the company's public news and information website.

Alexandria Engineering Journal (2022) 61, 113–124

HOSTED BY

Alexandria University

Alexandria Engineering Journal

www.elsevier.com/locate/aej
www.sciencedirect.com

A mathematical COVID-19 model considering asymptomatic and symptomatic classes with waning immunity

Nursanti Anggriani [a,*], Meksianis Z. Ndii [b], Rika Amelia [a], Wahyu Suryaningrat [a], Mochammad Andhika Aji Pratama [a]

[a] Department of Mathematics, Universitas Padjadjaran, Jln. Raya Bandung-Sumedang Km. 21 Jatinangor, Kab. Sumedang, 45363 Jawa Barat, Indonesia
[b] Department of Mathematics, Faculty of Sciences and Engineering, The University of Nusa Cendana, Kupang-NTT, Indonesia

Received 1 February 2021; revised 21 April 2021; accepted 27 April 2021
Available online 14 May 2021

KEYWORDS

COVID-19;
Basic Reproduction Ratio;
Waning immunity;
Asymptomatic;
Previous infection;
Parameter estimation

Abstract The spread of COVID-19 to more than 200 countries has shocked the public. Therefore, understanding the dynamics of transmission is very important. In this paper, the COVID-19 mathematical model has been formulated, analyzed, and validated using incident data from West Java Province, Indonesia. The model made considers the asymptomatic and symptomatic compartments and decreased immunity. The model is formulated in the form of a system of differential equations, where the population is divided into seven compartments, namely Susceptible Population (S_0), Exposed Population (E), Asymptomatic Infection Population (I_A), Symptomatic Infection Population (Y_S), Recovered Population (Z), Susceptible Populations previously infected (Z_0), and Quarantine population (Q). The results show that there has been an outbreak of COVID-19 in West Java Province, Indonesia. This can be seen from the basic reproduction number of this model, which is 3.180126127 ($\mathscr{R}_0 > 1$). Also, the numerical simulation results show that waning immunity can increase the occurrence of outbreaks; and a period of isolation can slow down the process of spreading COVID-19. So if a strict social distancing policy is enforced like a quarantine, the outbreak will lessen.

1. Introduction

The spread of COVID-19 has shocked society and currently has transmitted to more than 200 countries [1]. As of 04 April 2021, there are 130,998,190 confirmed cases, 2,853,280 death, and 105,447,782 recovered individuals [2]. It has caused severe economic and social loss. The disease has been transmitted

* Corresponding author at: Department of Mathematics, Universitas Padjadjaran, Jln. Raya Bandung-Sumedang Km. 21 Jatinangor, Kab. Sumedang 45363 Jawa Barat, Indonesia.
E-mail address: nursanti.anggriani@unpad.ac.id (N. Anggriani).

https://doi.org/10.1016/j.aej.2021.04.104
1110-0168

from human to human via droplets [3]. Infected individuals may show symptomps such as fever, cough, sore throat, rhinorrhea, myalgia or fatigue, phlegm, and headache [3–5] with the body temperature of 39°C or above [5]. Individuals who are infected by COVID-19 can show symptoms (symptomatic) or cannot show symptoms (asymptomatic) but both types of individuals can transmit disease [3]. The incubation period has been estimated between two fourteen days [6].

Research showed that there is possibility for infected individuals to be reinfected by COVID-19. Currently it has been found that several recovered individuals have been reinfected by COVID-19 and this can cause death from fatal heart failure [7]. Of the 111 recovered patients, 5% of China and 10% of South Korea tested positive for COVID-19 [8]. This situation contradicts the fact that after a person catches the virus and then recovers, the individual will forman antibody that prevents the same virus from attacking twice. Research showed that reinfected individuals have experienced viral replication but did not neutralize antibodies, which implies that it is unlikely that long-term protective immunity will occur in people with COVID-19 after the first infection [9]. The virus's immune response can be reduced within four months to one year after infection [10]. The genetic basis of the innate immune response affects the severity of COVID-19, it can also lead to more severe reinfection depending on antibodies generated against the bound virus but cannot neutralize the same strain [10]. The reinfection COVID-19 case has a more severe impact [11]. The reinfection occurs due to the decrease in the individual's immunity [12]. Understanding the effects of waning immunity is important.

Mathematical models can be used to understand the complex phenomena such as population dynamics problem [13–16] and disease transmission dynamics [17–21]. A compartment-based epidemic model in the form of system of (fractional or integer) differential equations has been formulated to understand disease transmission dynamics, where the human population is divided into different stages according to their status to the diseases [22–36]. A mathematical SEIR model is mostly used as a basis for the model's development for COVID-19 transmission [37,38]. The SEIR model has been extended to include quarantine compartment [39], to include symptomatic and asymptomatic classes [40]. The models are mostly used to investigate the disease transmission dynamics in several countries or provinces such as Indonesia [41], Hubei has been researched [42], Pakistan [43]. In this paper, a modified SEIR model considering symptomatic and asymptomatic cases from [44] has been formulated. The work focuses on studying the effects of waning immunity. The model is validated against data of COVID-19 incidence from West Java Province. The basic reproduction number is calculated, and a global sensitivity analysis is performed. The model is then used to determine he effects of waning immunity or reduced immunity to an increase in the number of infected individuals.

The remainder of this paper is organized as follows. In Section 2, the construction of the SEIR compartmental model. Next, the model's mathematical properties, such as the equilibrium points, Basic Reproduction Number, and the existence of backward bifurcation, are detailed in Section 3. In Section 4, we explain the real-world problem using the incidence data of West Java Province, Indonesia. A discussion on the Basic Reproduction Number and the sensitivity analysis results are provided in Section 5. Finally, some conclusions are presented in Section 6.

2. Model Formulation

We developed model of transmission of COVID-19 by considering asymptomatic and symptomatic compartments and decreased immunity. The total population is divided into Susceptible population (S_0), Exposed population (E), Asymptomatic infected population (I_A), Symptomatic infected population (Y_S), Recovered population (Z), Susceptible that previously infected (Z_0), Quarantine population (Q). The total number of population at time t is given by:

$$N(t) = S_0(t) + E(t) + I_A(t) + Y_S(t) + Z(t) + Z_0(t) + Q(t).$$

The assumption used in the formulation of a mathematical model for the spread of the COVID-19 disease is that individuals with symptoms will undergo hospitalization or quarantine. Deaths experienced by latent, symptomatic, asymptomatic, and quarantine individuals are caused by disease [45]. This means that the death of the three individuals is a combination of natural death and death due to disease. We assume that the μ_1 parameter contained in compartments E, I_a, Y_s is a death caused by COVID-19 plus a natural death factor. People who have decreased immunity can catch COVID-19 again with a high severity [11]. Hence, the second person infected will develop symptoms and be hospitalized. The model is represented by the diagrams shown in Fig. 1, with the description of the parameters given in Table 1.

So, based on the interaction diagram above, the COVID-19 spread mathematics model constructed as follows:

$$\frac{dS_0}{dt} = \Lambda - (\beta_1 I_A S_0 + \beta_2 Y_S S_0) - \mu S_0 \tag{1}$$

$$\frac{dE}{dt} = (\beta_1 I_A S_0 + \beta_2 Y_S S_0) - \alpha E - \mu_1 E \tag{2}$$

$$\frac{dI_A}{dt} = p\alpha E - \kappa I_A - \gamma_1 I_A - \mu_1 I_A \tag{3}$$

$$\frac{dY_S}{dt} = (1-p)\alpha E - qY_S - \gamma_2 Y_S + \beta_1 I_A Z_0 + \beta_2 Y_s Z_0 + \kappa I_A - \mu_1 Y_S \tag{4}$$

$$\frac{dZ}{dt} = \gamma_1 I_A + \gamma_2 Y_S + \delta Q - \xi Z - \mu Z \tag{5}$$

$$\frac{dZ_0}{dt} = \xi Z - \beta_1 I_A Z_0 - \beta_2 Y_s Z_0 - \mu Z_0 \tag{6}$$

$$\frac{dQ}{dt} = qY_S - \delta Q - \mu_1 Q, \tag{7}$$

with $S_0(0) \geqslant 0, E(0) \geqslant 0, I_A(0) \geqslant 0, Y_S(0) \geqslant 0, Z(0) \geqslant 0, Z_0(0) \geqslant 0, Q(0) \geqslant 0$as the initial conditions.

3. Mathematical Analysis

Lemma 3.1. If the initial values $S_0(0) > 0, E(0) > 0, I_A(0) > 0, Y_S\ (0) > 0, Z(0) > 0, Z_0(0) > 0$, and $Q(0) > 0$, the solution of

$$S_0(t), E(t), I_A(t), Y_S(t), Z(t), Z_0(t), Q(t),$$

of system Eqs. (1)–(7) are positif for all $t > 0$.

Proof. Assume that

$$\mathscr{X}(t) = \min\{S_0(t), E(t), I_A(t), Y_S(t), Z(t), Z_0(t), Q(t).\}, \forall t > 0.$$

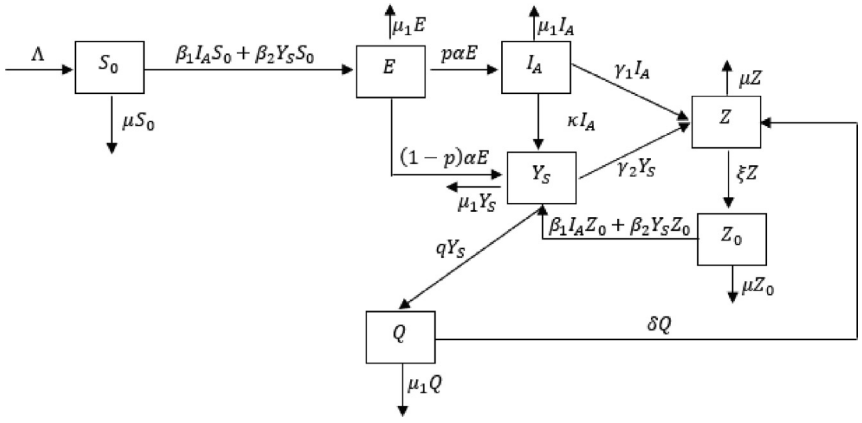

Fig. 1 Interaction Diagram of Populations.

Table 1 Parameters Description.

Parameters	Descriptions
Λ	The recruitment rate of susceptible population
β_1	The probability of transmission from asymptomatic infected people
β_2	The probability rate of transmission from symptomatic infected people
μ	The natural mortality rate
μ_1	Natural death rate plus COVID-19 death rate
α	The probability of exposed people become infected
p	The proportion of exposed people become infected
κ	The rate of asymptomatic infected people become infected symptomatic
q	The rate of quarantine
γ_1	The natural recovery rate of infected asymptomatic people
γ_2	The natural recovery rate of infected symptomatic people
δ	The recovery rate of quarantine people
ξ	The probability rate of recovered people become susceptible (*waning immune*)

Clearly, $\mathscr{X}(0) > 0$.

Assuming that there exist a $t_1 > 0$ such that.

$\mathscr{X}(t_1) = 0$ and $\mathscr{X}(t) > 0$, for all $t \in [0, t_1)$,

If $\mathscr{X}(t_1) = S_0(t_1)$, then $E(t) \geqslant 0, I_A(t) \geqslant 0, Y_S(t) \geqslant 0, Z(t) \geqslant 0, Z_0(t) \geqslant 0$ for all $t \in [0, t_1]$.

From the equation of model (1), we can obtain

$$\frac{dS_0}{dt} \geqslant -\beta_1 I_A S_0 - \beta_2 Y_S S_0 - \mu S_0, t \in [0, t_1].$$

Thus, we have

$$S_0(t) \geqslant S_0(0) \exp\left(-\int_0^{t_1} [\beta_1 I_A S_0 + \beta_2 Y_S S_0 + \mu S_0] dt\right),$$

which will be positive since exponential functions and initial solutions $S_0(0)$are non-negative. Thus, $S_0(t) > 0$ for all $t \geqslant 0$.

Similarly, we can also prove that

$$E(t) > 0, I_A(t) > 0, Y_S(t) > 0, Z(t) > 0, Z_0(t) > 0, Q(t) > 0.$$

Lemma 3.2. All solution of system Eqs. (1)–(7) are bounded for all $t \in [0, t_0]$

Proof. Since $N(t) = S_0(t) + E(t) + I_A(t) + Y_S(t) + Z(t) + Z_0(t) + Q(t)$.

We get:

$$\frac{dN}{dt} = \Lambda - \mu(S_0 + Z + Z_0) - \mu_1(E + I_A + Y_S + Q).$$

Assume that $\mu = \mu_1$, to simplify the analysis process.

Then:

$$\frac{dN}{dt} = \Lambda - \mu N.$$

Thus we have

$$0 \leqslant \limsup_{t \to \infty} N(t) \leqslant \frac{\Lambda}{\mu},$$

so all solutions of system Eqs. (1)–(7) are ultimately bounded for all $t \in [0, t_0]$.

3.1. Non-endemic Equilibrium Point

The non-endemic equilibrium point of the COVID-19 disease model is obtained by setting $I_A = 0, E = 0, Y_S = 0$, and substituting it into Eqs. (1)–(7) to obtain:

$$\begin{aligned} P_0 &= (S_0^0, E^0, I_A^0, Y_S^0, Z^0, Z_0^0, Q^0) \\ &= \tfrac{\Lambda}{\mu}, 0, 0, 0, 0, 0, 0) \end{aligned} \tag{8}$$

3.2. Stability of Non-endemic Equilibrium Point

Theorem 3.3. The non-endemic equilibrium point of system Eqs. (1)–(7) is locally asymptotically stable whenever it exists.

Proof. By following Diekmann (2000) [46] substituting P_0 from 8 into the Jacobian matrix for the non-endemic equilibrium point is obtained:

$$J(P_0)=\begin{bmatrix} -\mu & 0 & \frac{-\beta\Lambda}{\mu} & \frac{-\beta\Lambda}{\mu} & 0 & 0 & 0 \\ 0 & -\alpha-\mu & \frac{\beta\Lambda}{\mu} & \frac{\beta\Lambda}{\mu} & 0 & 0 & 0 \\ 0 & p\alpha & -\kappa-\gamma_1-\mu_1 & 0 & 0 & 0 & 0 \\ 0 & (1-p)\alpha & \kappa & -q-\gamma_2-\mu_1 & 0 & 0 & 0 \\ 0 & 0 & \gamma_1 & \gamma_2 & -\xi-\mu & 0 & \delta \\ 0 & 0 & 0 & 0 & \xi & -\mu & 0 \\ 0 & 0 & 0 & q & 0 & 0 & -\delta-\mu_1 \end{bmatrix}.$$

The characteristics of the polynomial is

$$\mathscr{P}(\lambda)=\frac{1}{\mu}((\lambda+\mu)\mathscr{P}_1(\lambda))=0, \tag{9}$$
$$\mathscr{P}_1(\lambda)=a_0\lambda^6+a_1\lambda^5+a_2\lambda^4+a_3\lambda^3+a_4\lambda^2+a_5\lambda+a_6.$$

From the polynomial $(\mathscr{P}(\lambda))$ we get $\lambda_1=-\mu$ and for λ_i with $i=2,3,\ldots,7$ will be negative if $a_j>0$ where $j=0,1,2,\ldots,6, \mathscr{R}_0<1, a_1a_2>a_0a_3, a_1(a_2a_3+a_0a_5)>a_1^2a_4+a_0a_3^2$, and $a_1a_2a_4>a_0(a_1a_6+a_2a_5)$. Since the coefficients in the characteristic equation $\mathscr{P}_1(\lambda)$ are complex, we proceed to analyze the coefficient values numerically with $\beta_1=\beta_2$. The results of the numerical analysis obtained (see **Appendix A.**), show that for λ_i with $i=2,3,\ldots,7$ negative. Because λ_j with $j=1,2,3,\ldots,7$ is negative, it can be concluded that the non-endemic equilibrium point of the system (1–7) is locally stable, so **Theorem 3.3** is proven.

3.3. Basic Reproduction Ratio

The Basic Reproduction Ratio $(\mathscr{R}_0)$ is an important number in epidemiology, which is defined as the number of secondary infections caused by one primary infection in a population. We use the next-generation method to determine $\mathscr{R}_0$, the value of $\mathscr{R}_0$ an be obtained by finding the dominant eigenvalue FV^{-1}. Where F and V are Jacobian matrices of f (newly infected matrices) and v (exiting matrices) that are evaluated at the disease-free equilibrium point (P_0) from 8. From the models (1–7) are obtained:

$$F=\begin{bmatrix} 0 & \frac{\Lambda\beta_1}{\mu} & \frac{\Lambda\beta_2}{\mu} \\ 0 & 0 & 0 \\ 0 & 0 & 0 \end{bmatrix},$$

$$V=\begin{bmatrix} -\alpha-\mu & 0 & 0 \\ \alpha p & -\kappa-\gamma_1-\mu & 0 \\ (1-p)\alpha & \kappa & -q-\gamma_2-\mu_1 \end{bmatrix}$$

and

$$FV^{-1}=\begin{bmatrix} -\frac{\alpha(((p-1)\beta_2-p\beta_1)\mu_1+(\gamma_1 p-\kappa-\gamma_1)\beta_2-p\beta_1(\gamma_2+q))\Lambda}{\mu(\mu_1+\alpha)(\mu_1+\kappa+\gamma_1)(\gamma_2+q+\mu_1)} & \frac{\Lambda(\beta_1(\gamma_2+q+\mu_1)+\beta_2\kappa)}{\mu(\gamma_2+q+\mu_1)(\mu_1+\kappa+\gamma_1)} & \frac{\Lambda\beta_2}{\mu(\gamma_2+q+\mu_1)} \\ 0 & 0 & 0 \\ 0 & 0 & 0 \end{bmatrix}.$$

The eigenvalues of (FV^{-1}) are:

$$\lambda_1=-\frac{\alpha(((p-1)\beta_2-p\beta_1)\mu_1+(\gamma_1 p-\kappa-\gamma_1)\beta_2-p\beta_1(\gamma_2+q))\Lambda}{\mu(\mu_1+\alpha)(\mu_1+\kappa+\gamma_1)(\gamma_2+q+\mu_1)}, \lambda_{2,3}=0.$$

Following the method described by Castilo Chavez et al. (2002) [47] the basic reproduction number in the COVID-19 is:

$$\mathscr{R}_0=\xi(FV^{-1})=-\frac{\alpha(((p-1)\beta_2-p\beta_1)\mu_1+(\gamma_1 p-\kappa-\gamma_1)\beta_2-p\beta_1(\gamma_2+q))\Lambda}{\mu(\mu_1+\alpha)(\mu_1+\kappa+\gamma_1)(\gamma_2+q+\mu_1)}.$$

Under certain conditions where the probability of transmission from infected people same as from asymptomatic infected people hold $\beta_1=\beta_2$ and the natural recovery rate of infected people asymptomatic and symptomatic $\gamma_1=\gamma_2=\gamma$. It obtained the reproduction number for this condition symbolized by $\mathscr{R}_{0\beta}$. Where:

$$\mathscr{R}_{0\beta}=\frac{\Lambda\alpha\beta(pq+\mu_1+\gamma+\kappa)}{\mu(\mu_1+\gamma+\kappa)(\mu_1+\alpha)(\mu_1+\gamma+q)}.$$

3.4. Endemic Equilibrium Points

Theorem 3.4. An endemic equilibrium point of system

$P_1=(S_0^*,E^*,I_A^*,Y_S^*,Z^*,Z_0^*,Q^*)$ will exist if $\mathscr{G}>0$ and $\mathscr{H}>0$ or $\mathscr{G}<0$ and $\mathscr{H}<0$.

Proof. The endemic point of this disease is endemic in certain areas for a certain period, which releases the COVID-19 in the population. It is indicated by the presence of compartments exposed to virus transmission E^*, I_a^*, Y_S^* at steady state. By calculating model ((1), (5)–(7)) and setting the right hand side zero we obtained:

$$S_0^*=\frac{\Lambda}{\beta(I_A^*+Y_S^*)+\mu},$$
$$I_A^*=\frac{\alpha Ep}{\gamma+\kappa+\mu_1},$$
$$Y_S^*=\frac{(1-p)\alpha E^*+\beta I_A^* Z_0^*}{q+\gamma-\beta Z_0^*},$$
$$Z^*=\frac{\gamma(I_A^*+Y_S^*)+\delta Q^*}{(\mu+\xi)},$$
$$Z_0^*=\frac{\xi Z^*}{(\beta(I_A^*+Y_S^*)+\mu},$$
$$Q^*=\frac{qY_S^*}{\delta+\mu_1}.$$

By substituting $S_0^*, I_A^*, Y_S^*, Z_0^*, Z_0^*, Q^*$ to equation (2.2) and set the right hand side equal to zero, obtained:

$$A_2E^2+A_1E+A_0=0, \tag{10}$$

which this polynomial have to roots $E=0$ or $E=E^*$ which can be written by

$$E^*=\frac{\mathscr{G}}{\mathscr{H}},$$

where $\mathscr{G}$ and $\mathscr{H}$ written on **Appendix B**.

Because the denomerator of $\mathscr{H}$ always positif, the steady state E^* will exsist if $R_{0\beta}>1$ and $pq>0$, see attachment for the proof. The system of Eqs. (1)–(7) will have an endemic equilibrium point if $\mathscr{G}>0$ and $\mathscr{H}>0$ or $\mathscr{G}<0$ and $\mathscr{H}<0$. This condition indicates that the system of Eqs. (1)–(7) has a unique endemic equilibrium point.

3.5. Stability of Endemic Equilibrium Point

Theorem 3.5. The endemic equilibrium point of the system (P_1) is locally asymptotically stable whenever it exists.

Proof. Following method on the proof of Theorem 3.5, Based on the method of proof of Theorem 2, by substituting P_1 is obtained characteristic polynomial

$$\mathscr{Q}(\lambda)=a_0\lambda^7+a_1\lambda^6+a_2\lambda^5+a_3\lambda^4+a_4\lambda^3+a_5\lambda^2+a_6\lambda+a_7. \tag{11}$$

From the polynomial ($\mathcal{Q}(\lambda)$) we get λ_i with $i = 1, 2, 3, \ldots, 7$ will be negative if $a_j > 0$ where $j = 0, 1, 2, \ldots, 7, a_1a_2 > a_0a_3$, $a_1(a_2a_3 + a_0a_5) > a_1^2a_4 + a_0a_3^2, a_1a_2(a_3a_4 + a_0a_7) > a_0a_3(a_1a_6 + a_2a_5)$, and $a_2a_5 > a_0a_7$. Since the coefficients in the characteristic equation $\mathcal{Q}(\lambda)$ are complex, we proceed to analyze the coefficient values numerically. The results of the numerical analysis obtained can be seen in the **Appendix C.** It satisfies the Routh-Hurwitz's criteria so that the endemic point is locally asymptotically stable whenever it exists. These results will remain consistent using the parameter values in Table 2.

3.6. Global Stability of The Equilibria

Theorem 3.6. The non-endemic equilibrium point (P_0) is globally asymptotically stable if
$\frac{\beta_1\Lambda}{\mu} < \mu_1 \text{and} \frac{\beta_2\Lambda}{\mu} < \mu_1.$

Proof. Refer to global proving by Tewa et al. (2009)[48], let

$P_0 = (S_0{}^0, E^0, I_A^0, Y_S^0, Z^0, Z_0^0, Q^0) = \left(\frac{\Lambda}{\mu}, 0, 0, 0, 0, 0, 0\right)$ is the non-endemic equilibrium point of system Eqs. (1)–(7).

Define the Lyapunov function

$$V(t) = \left(S_0 - S_0^* - S_0^* \frac{\ln S_0}{S_0^*}\right) + E + I_A + Y_S + Z + Z_0 + Q.$$

Differentiating with respect to time yields

$$\begin{aligned}
\frac{dV}{dt} &= (S_0 - S_0^*)\frac{\frac{dS_0}{dt}}{S_0^*} + \frac{dE}{dt} + \frac{dI_A}{dt} + \frac{dY_S}{dt} + \frac{Z}{dt} + \frac{Z_0}{dt} + \frac{Q}{dt} \\
\frac{dV}{dt} &= \frac{(S_0 - S_0^*)(\Lambda - \mu S_0)}{S_0^*} - (S_0 - S_0^*)(\beta_1 I_A + \beta_2 Y_S) + \beta_1 I_A S_0 + \beta_2 Y_S S_0 \\
&\quad -\alpha E - \mu_1 E + p\alpha E - \kappa I_A - \gamma I_A - \mu_1 I_A + (1-p)\alpha E - qY_S - \gamma Y_S \\
&\quad +\beta_1 I_A Z_0 + \beta_2 Y_S Z_0 + \kappa I_A - \mu_1 Y_S + \gamma I_A + \gamma Y_S + \delta Q - \xi Z - \mu Z \\
&\quad +\xi Z - \beta_1 I_A Z_0 - \beta_2 Y_S Z_0 - \mu Z_0 + qY_S - \delta Q - \mu_1 Q \\
\frac{dV}{dt} &= \frac{(S_0 - S_0^*)(\Lambda - \mu S_0)}{S_0} - (S_0 - S_0^*)(\beta_1 I_A + \beta_2 Y_S) + \beta_1 I_A S_0 + \beta_2 Y_S S_0 \\
&\quad -\mu_1(E + I_A + Y_S + Q) - \mu(Z + Z_0) \\
\frac{dV}{dt} &= \Lambda(S_0 - S_0^*)\left(\frac{1}{S_0} - \frac{1}{S_0^*}\right) + (\beta_1 S_0^* - \mu_1) I_A + (\beta_2 S_0^* - \mu_1) Y_S - \mu_1(E + Q) \\
&\quad -\mu(Z + Z_0) \\
\frac{dV}{dt} &= \Lambda(S_0 - S_0^*)\left(\frac{1}{S_0} - \frac{1}{S_0^*}\right) + \left(\frac{\beta_1\Lambda}{\mu} - \mu_1\right) I_A + \left(\frac{\beta_2\Lambda}{\mu} - \mu_1\right) Y_S - \mu_1(E + Q) \\
&\quad -\mu(Z + Z_0).
\end{aligned}$$

The value of $\frac{dV}{dt}$ will be negative if

$\frac{\beta_1\Lambda}{\mu} < \mu_1 \text{and} \frac{\beta_2\Lambda}{\mu} < \mu_1.$

By following LaSalle's extension on Lyapunov's method [49], disease-free equilibrium P_0 is globally asymptotically stable.

This concludes the proof.

Table 2 Parameters Values.

Parameter	Value	Unit	Source
Λ	$\frac{10^7}{365\times65}$	$people \times day^{-1}$	Estimated
β_1	1.727×10^{-7}	$(people \times day)^{-1}$	Fitting
β_2	7.478×10^{-8}	$(people \times day)^{-1}$	Fitting
μ	$\frac{1}{365\times65}$	day^{-1}	Estimated
μ_1	0.082	day^{-1}	Fitting
α	$\frac{1}{5.2}$	day^{-1}	[52]
p	0.2	N/A	Assumed
κ	0.19	day^{-1}	[53]
q	1.026×10^{-6}	day^{-1}	Fitting
γ_1	$\frac{1}{10}$	day^{-1}	[52]
γ_2	$\frac{1}{14}$	day^{-1}	Assumed
δ	0.1	day^{-1}	[54]
ξ	0.02	day^{-1}	Assumed

4. Sensitivity Analysis

This section presents a global sensitivity analysis of the model. We use the combination of Latin Hypercube Sampling (LHS) and Partial Rank Correlation Coefficient (PRCC) to determine the most influential parameters of the model [50]. LHS is stratified sampling without replacement. The parameter distribution is divided into equation probability intervals and then is sampled. Each parameter interval is sampled once and the entire range of each parameter is explored. A matrix is then generated which consists of N rows for the number of samples and k columns for the number of varied parameters. The model solution is then generated using the combination of parameters (each row). The outcome of interest is the increasing number of infected individuals. The result of sensitivity analysis is given in Fig. 2.

It showed that the waning immunity (ξ) is one of the influential parameters. When the value of waning immunity increases, the number of infected individuals also increases. This means that waning immunity would contribute to the increasing number of infected individuals. Therefore, an analysis of effects of waning immunity is of importance. The parameters k, p are also influential and has positive relationship. This means that the rate of asymptomatic become infected and the proportion of exposed individuals become infected contributes to an increasing number of infected individuals. When these parameter values increases, the number of infected individuals decreases.

5. A Case Study

In this section, we estimated the parameters β_1, β_2, and γ against data of West Java, Indonesia. The data are obtained from the website https://pikobar.jabarprov.go.id/table-case/. We estimate the parameter values by minimizing the sum of squared error. The parameters b and a are estimated against the data for the first 30 days. It is sufficient since the aim is to obtain the general insights of the values of parameters β_1, β_2 and q in the early period of the outbreak. The other parameter values are obtained from literature and are given in Table 2.

The lsqnonlin built-in function in MATLAB is used for the parameter estimation.

We minimize the sum of squared error as

$$SE = \sum_{t=1}^{n} (Q_t - g_t(x))^2. \tag{12}$$

where Q_t is the number of active cases of Q up to day t, respectively, while $g_t(x)$ is the number of active cases for Q up to day t from the model's solution, respectively. The transmission rate, β_0 and β_1, the quarantine rate q are then estimated using the "lsqnonlin" built-in function in MATLAB. The case fatality rate is estimated using the linear regression method.

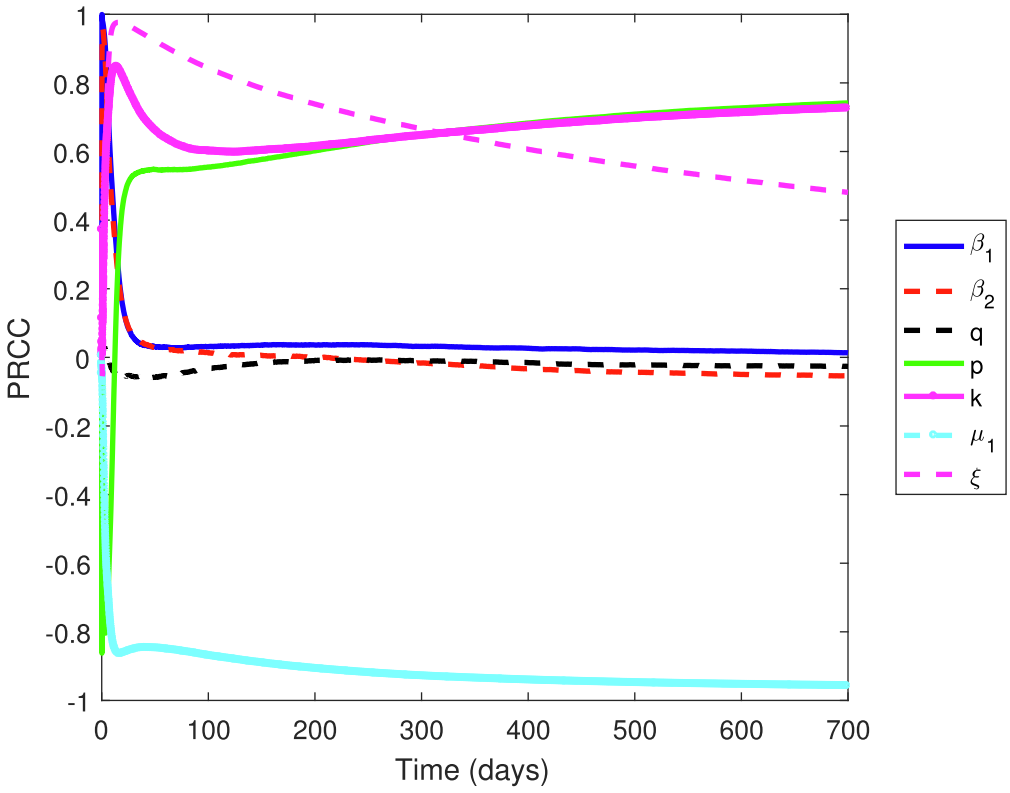

Fig. 2 PRCC over time when we measure against the increasing number of infected individuals.

The initial conditions used Table 3. The initial conditions for susceptible individuals are an approximate total population in West Java. The fitted values of β_1, β_2 and q. The values are then used in the numerical simulation. The plot of model's solution and data is given in Fig. 3. With these parameter values, the reproduction number for West Java $\mathcal{R}_0 = 3.180126127$. This means that an outbreak happens and the control needs to be implemented to minimize the risk of infections.

6. Numerical Simulation

This numerical simulation is designed to support the results of the analysis discussed in the previous section. We set the parameter by curve fitting from actual case of COVID-19 in West Java Province, Indonesia. We applied Runge–Kutta-Fehlberg (RKF) method in MAPLE software, to solve the ordinary differential equations of model Eqs. (1)–(7) using the parameters in Tables 2 and 3. RKF method is one of the

Table 3 Initial Values of each Compartments.

Compartment	$S(0)$	$E(0)$	$Ia(0)$	$Ys(0)$	$Z(0)$	$Z_0(0)$	$Q(0)$
Initial Values	10^7	100	100	100	100	100	5

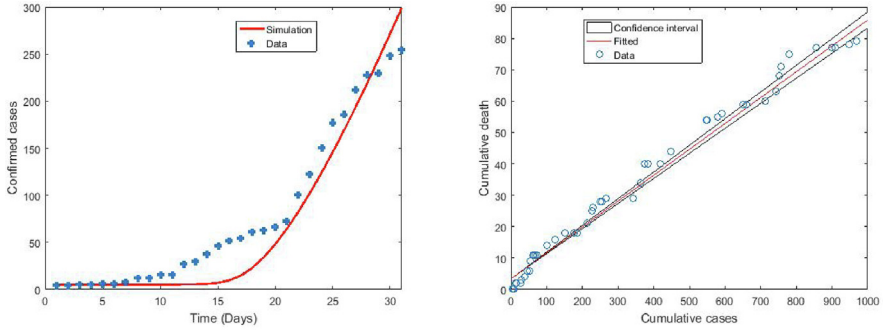

(a) (b)

Fig. 3 Fitting Parameter from Confirmed Cases (**a**) and Cumulative Death (**b**).

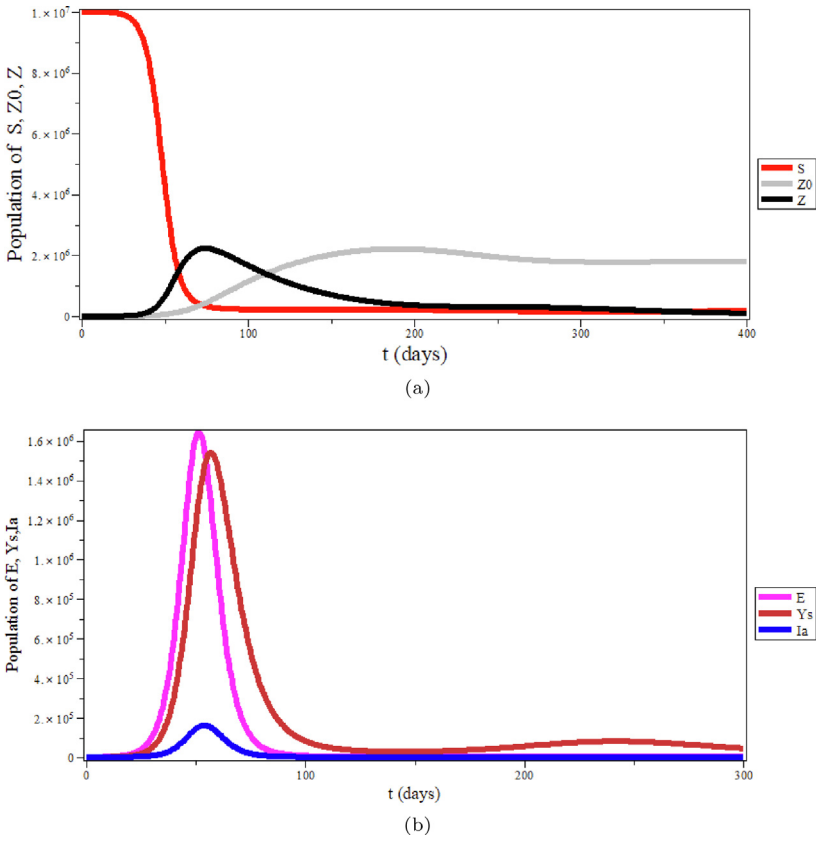

Fig. 4 Dynamical Population of each Compartment: **(a)** Population of $S, Z0, Z$ **(b)** Population of E, Ys, & Ia.

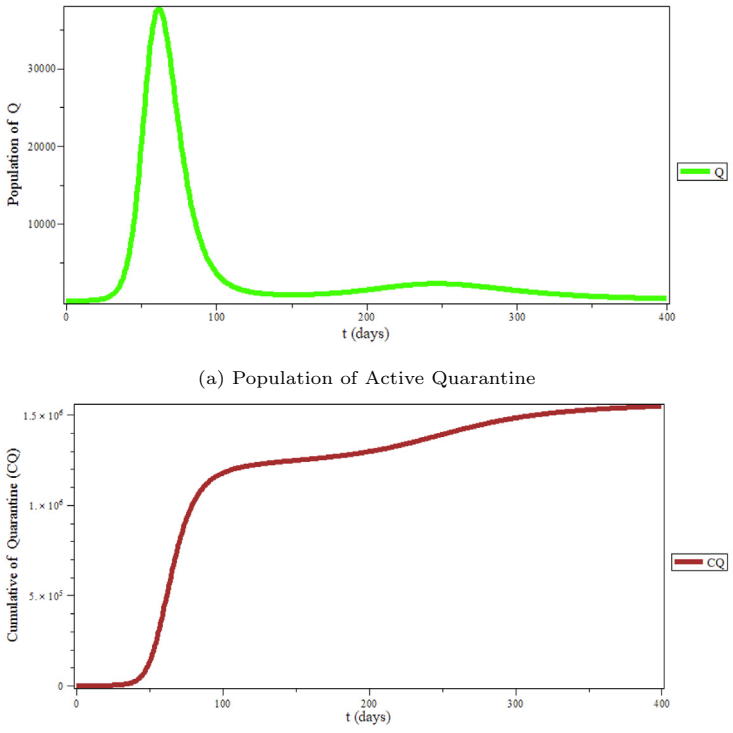

Fig. 5 Dynamical Population of **(a)** Active Quarantine **(b)** Cumulative Quarantine.

most popular numerical approach because it is quite accurate, stable, to program [51].

Fig. 4 show the endemic incidence where the susceptible population (S_0) decreases as a result of transmission from the symptomatic and asymptomatic infected population. Hereafter, this increases the latent population (E), the asymptomatic infected population (I_A), the symptomatic infected population (Y_S), the recovered population (Z), the susceptibility to previously infected populations (Z_0), and the quarantine population (Q).

However, after the 20^{th} day, the latent (E) and asymptomatic infected population (I_A) decreased, this is because the latent population and the asymptomatic infected population became the removed population. While symptomatic human populations (Y_S) have declined due to an increase in quarantined populations (Q), the recovered (Z) and susceptible that previously infected populations (Z_0) have consequently increased.

Fig. 5 shows the number of quarantine population Q and the cumulative population of quarantine. The number of quarantine compartment populations increases as the asymptomatic infection increases. The peak occurs at 30 days where the number reaches 70 and after that decreases. At the end of the 400^{th} day, the number of cumulative quarantine reaches 3200.

6.1. The Effect of Waning Immunity

In this section, we simulate the sensitivity analysis for the effect of parameter ξ, related to waning immunity issue, which describes the probability rate of recovered people become susceptible, and the probability rate of susceptible people that previously infected become asymptomatic infected, respectively. Using the parameters and initial values in Tables 2 and 3, except for ξ, we choose $\xi = 0.001, 0.01, 0.1, 1$.

Figs. 6 and 7 show the effect of increasing the value of ξ and τ. In these simulations the peak time of disease spread do not change, but at the time after the peak has been passed, the more value of ξ and τ multiply the number of Asymptomatic infected population (Y_S).

The effect of changes in the value of the probability rate of recovered people become susceptible (ξ) on the E, I_A, Y_S, and Z compartments is shown in Fig. 7. The changes value of the parameter ξ did not have a significant impact on the number of compartments E and I_A. The number of populations $E(t)$ and $I_A(t)$ is relatively unchanged for every $\xi \in [0.001, 0.1]$. This means that changes in the reinfected parameter value do not really affect the number population Exposed (E) and asymptomatic infected population (I_A).

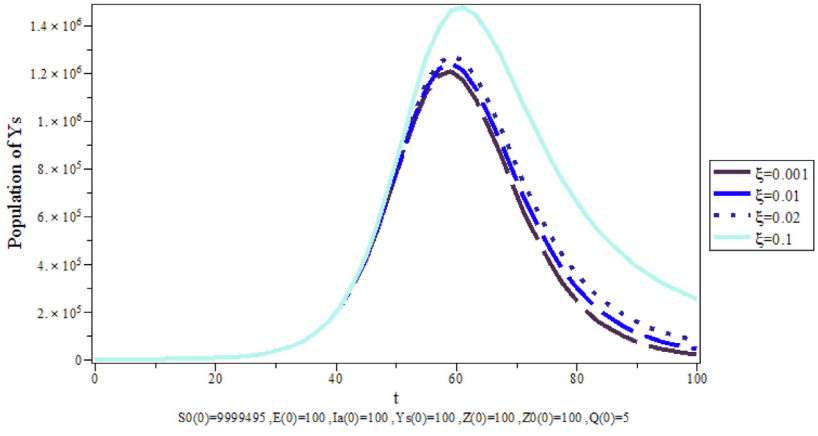

(a) Population of Active Quarantine

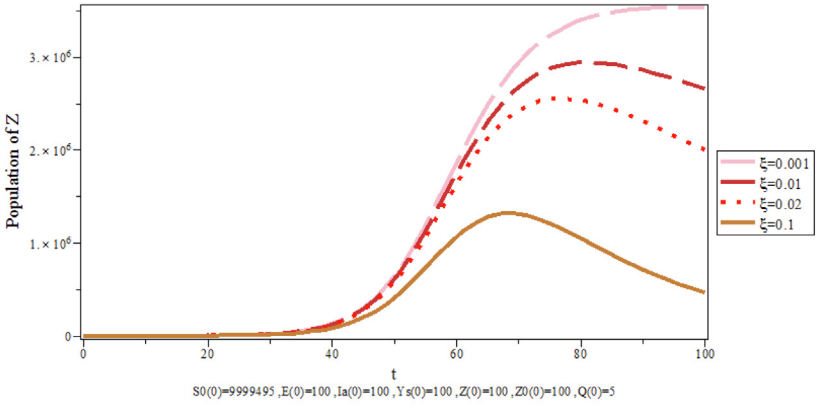

(b) Population of Cumulative Quarantine

Fig. 6 Simulation of The effect of Waning Immunity (ξ) on **(a)**Symptomatic Infected Population (Y_S) and **(b)** Quarantine Population (Q).

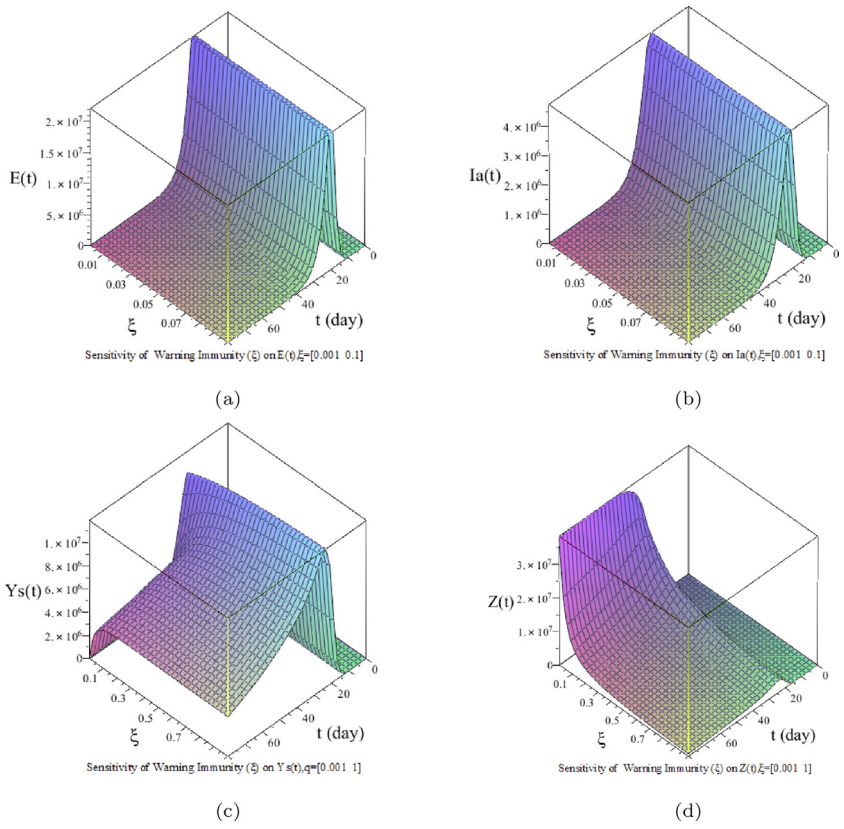

Fig. 7 Simulation of The effect of Waning Immunity ξ with respect to time (t) for each Compartments (**a**) E, (**b**) I_A, (**c**) Y_S, and (**d**) Z.

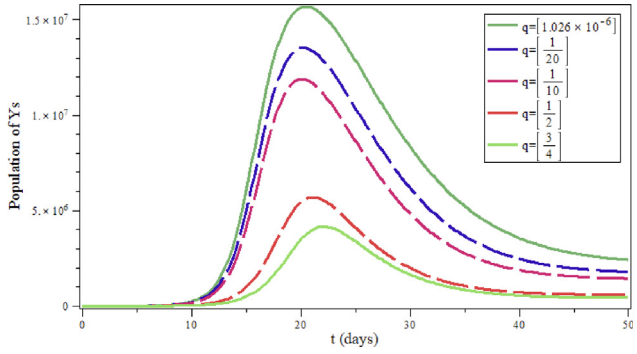

Fig. 8 Dynamical population of Symptomatic Infected Population (Y_S) in changes of quarantine parameter (q).

However, the higher the value of the parameter ξ, the higher the population of Y_S after passing the peak of the spread, and the lower the population Z. When this parameter is greater, the recovered population (Z) decreases due to the loss of immunity and returns to the susceptible population that previously infected (Z_0). Where population Z_0 can be re-infected to become asymptomatic infected population (Y_S).

6.2. The Effect of Quarantine

Fig. 8 show that with increase the value of quarantine parameter (q), the peak size and the final size of symptomatic infected population (Y_S) is decrease. This show that Increasing the intensity of quarantine policy may press the spread of COVID-19. Fig. 9 show that changes in the value of quarantine parameters to the population of each compartments E, I_A, Y_S, and Z are presented in 3-dimensional changes in time. When the value of the quarantine parameter q is increased, within the range $[0.01, 1]$, the number of infected populations can be reduced. This is indicated by the reduction in the peak value of Exposed (E), Asymptomatic Infected (I_A), and Symptomatic Infected (Y_S), in the change in the value of q. Meanwhile the population in the quarantine compartment (Q) is increasing from population of Symptomatic Infected which did Quarantine.

7. Discussion and Conclusion

We have formulated a mathematical model of COVID-19 transmission by considering infected individuals with symptoms and asymptomatic, as well as decreased immunity, validated with data from West Java Province, Indonesia. The compartment-based model is formulated as a system of differential equations, where the population is divided into Susceptible Populations (S_0), Exposed Populations (E), Asymptomatic Infection Populations (I_A), Symptomatic Infection Populations (Y_S), Recovered Populations (Z), Susceptible Populations previously infected (Z_0), and Quarantine Population (Q). Then the model is analyzed mathematically, the results show that there are two equilibrium points, namely a disease-free equilibrium point and an endemic equilibrium point. Besides, with the next-generation matrix method, the Basic Reproduction Number ($\mathscr{R}_0$) for West Java Province is obtained of 3.180126127. This means that West Java Province is affected by the COVID-19 outbreak and controls are needed to minimize the risk of transmitting COVID-19. Stability and

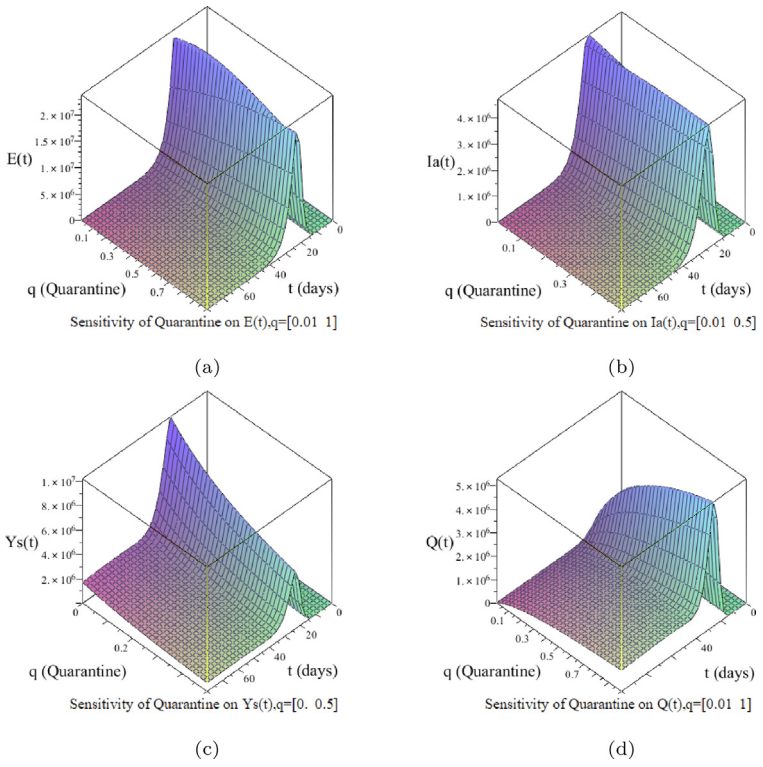

Fig. 9 Simulation of The effect of quarantine parameter (q) with respect to time (t) for each Compartments (**a**) E, (**b**) I_A, (**c**) Y_S, and (**d**) Q.

sensitivity are analyzed to determine the parameters that influence the spread of COVID-19. The simulation results show that the factor of decreasing immunity can affect the spread of COVID-19. This is because when the increase in immunity decreases, the infected population increases. Meanwhile, reinfection has no significant effect on the number of exposed and infected asymptomatic populations and the isolation period can slow the spread of COVID-19 in West Java Province, Indonesia. The results obtained can be used as a reference for the early prevention of the spread of COVID-19 in West Java.

8. Authors's Contributions

N Anggriani, R Amelia, & W Suryaningrat contributed to the study design, model formulation, model analysis, and numerical simulation. MZ Ndii designed sensitivity analysis and performed the case study including parameter estimation. MAA Pratama complete and verify the analysis. All authors have read and agreed to the published version of the manuscript.

Declaration of Competing Interest

The authors declare that they have no known competing financial interests or personal relationships that could have appeared to influence the work reported in this paper.

Acknowledgments

The work was supported by Universitas Padjadjaran, with contract number 1735/UN6.3.1/LT/2020 through Hibah Riset Data Pustaka dan Daring.

Appendix A. Proof of Numerical Analysis of Theorem 3.3

Coefficient polynomial ($\mathscr{P}_1(\lambda)$):

$a_0 = 1,$
$a_1 = 1.030393017,$
$a_2 = 0.3892774217,$
$a_3 = 0.06516694579,$
$a_4 = 0.004442996019,$
$a_5 = 0.00006597971860, \&$
$a_6 = 2.773132296 \times 10^{-9}$

Value of:

$a_1 a_2 = 0.4011087370,$
$a_0 a_3 = 0.06516694579,$
$a_1(a_2 a_3 + a_0 a_5) = 0.4683242878,$
$a_1^2 a_4 + a_0 a_3^2 = 0.008963903101,$
$a_1 a_2 a_4 = 0.001782124518,$
$a_0(a_1 a_6 + a_2 a_5) = 0.00002568727211.$

Appendix B. Characteristic Polynomial of Exposed Compartment

$$\mathscr{G} = \sqrt{\mathscr{K}} + (((-\mu_1^2\gamma + ((-q-\gamma)\delta - \kappa\gamma - \gamma^2)\mu_1 + (-\gamma^2 + (-\kappa - q)\gamma - \kappa q)\delta)\mu + \beta\Lambda\mu_1^2 + (\delta\beta\Lambda + \Lambda\beta\gamma + (\kappa + qp)\Lambda\beta)\mu_1 + (\Lambda\beta\gamma + (2qp + \kappa)\Lambda\beta)\delta)\xi + (\beta\Lambda\mu_1^2 + (\delta\beta\Lambda + \Lambda\beta\gamma + (\kappa + qp)\Lambda\beta)\mu_1 + (\Lambda\beta\gamma + (\kappa + qp)\Lambda\beta)\delta)\mu)\alpha + (-\mu_1^3\gamma + ((-q-\gamma)\delta - \kappa\gamma - \gamma^2)\mu_1^2 + (-\gamma^2 + (-\kappa - q)\gamma - \kappa q)\delta\mu_1)\mu\xi,$$

where

$$\mathscr{K} = ((\mu_1\gamma + (q+\gamma)\delta)^2(\kappa+\gamma+\mu_1)^2(\alpha+\mu_1)^2\xi^2 + 2(\kappa+\gamma+\mu_1)(\delta+\mu_1)\beta\Lambda\alpha(\alpha+\mu_1)$$
$$(-\mu_1^2\gamma + ((-\gamma+(2p-1)q)\delta - \gamma(\kappa+\gamma+qp))\mu_1 + \delta(q+\gamma)(qp-\kappa-\gamma))\xi$$
$$+\beta^2\alpha^2\Lambda^2(\delta+\mu_1)^2(\kappa+\gamma+qp+\mu_1)^2)\mu^2 + 2\xi\beta\Lambda\alpha((\kappa+\gamma+\mu_1)(-\mu_1^3\gamma +$$
$$((-2\gamma+(2p-1)q)\delta - \gamma(\kappa+\gamma+qp))\mu_1^2 + ((-\gamma+(2p-1)q)\delta - 2\gamma^2$$
$$+((-p-1)q-2\kappa)\gamma + q(qp-\kappa))\delta\mu_1 - \delta^2(\kappa+\gamma)(q+\gamma))(\alpha+\mu_1)\xi$$
$$+(\mu_1{}^2 + (\kappa+\gamma+\delta+qp)\mu_1 + \delta(\kappa+\gamma))(\delta+\mu_1)\beta\Lambda\alpha(\kappa+\gamma+qp+\mu_1))\mu$$
$$+\xi^2(\mu_1{}^2 + (\kappa+\gamma+\delta+qp)\mu_1 + \delta(\kappa+\gamma))^2\beta^2\Lambda^2\alpha^2,$$

and

$$\mathscr{H} = \{2\alpha\beta\delta pq\xi(\mu_1+\alpha)\}.$$

By substituting the parameter value from Table 2 we have endemic equilibrium point:

$$E = 1536.477836,$$
$$I_A = 158.8583370,$$
$$Q = 0.01936422900,$$
$$S_0 = 679.0681919,$$
$$Y_S = 3434.980193,$$
$$Z = 17931.49917,$$
$$Z_0 = 577.7849236.$$

So, the non-endemic equilibrium point is stable if it exists, because it satisfies Routh-Hurwit's criterion. These results remain consistent using the parameter values in the Table 2, except $\beta_1 = \beta_2 = 0.7477942169036 \times 10^{-10}$.

Appendix C. Proof of Numerical Analysis of Endemic Equilibrum Point

Coefficient polynomial ($\mathscr{Q}(\lambda)$):

$$a_0 = 1.000000000,$$
$$a_1 = 2.171964310,$$
$$a_2 = 1.885854850,$$
$$a_3 = 0.84368388,$$
$$a_4 = 0.20819336,$$
$$a_5 = 0.0279316,$$
$$a_6 = 0.001468969,$$
$$a_7 = 0.00001178844740.$$

Value of:

$$a_1a_2 = 4.096009428,$$
$$a_0a_3 = 0.8436838800,$$
$$a_1(a_2a_3 + a_0a_5) = 3.516403565,$$
$$a_1^2a_4 + a_0a_3^2 = 1.693939876,$$
$$a_1a_2(a_3a_4 + a_0a_7) = 0.7195098093,$$
$$a_0a_3(a_1a_6 + a_2a_5) = 0.04713281469,$$
$$a_2a_5 = 0.05267494333,$$
$$a_0a_7 = 0.00001178844740.$$

References

[1] Q. Li, X. Guan, P. Wu, X. Wang, L. Zhou, Y. Tong, Z. Feng, Early transmission dynamics in Wuhan, China, of novel coronavirus-infected pneumonia, New England journal of medicine. 382 (2020) 1199–1207.

[2] Worldometer, COVID-19 coronavirus pandemic, (2020). Avaliable from: https://www.worldometers.info/coronavirus/.

[3] J.F.W. Chan, S. Yuan, K.H. Kok, K.K.W. Yo, H. Chu, et al, A familial cluster of pneumonia associated with the 2019 novel coronavirus indicating person-to-person transmission: a study of a family cluster, Lancet 395 (2020) (2019) 514–523.

[4] N. Chen, M. Zhou, X. Dong, J. Qu, F. Gong, et al, Epidemiological and clinical characteristics of 99 cases of 2019 novel coronavirus pneumonia in Wuhan, China: a descriptive study, Lancet 395 (2020) (2019) 507–513.

[5] C. Huang, Y. Wang, X. Li, L. Ren, J. Zhao, et al, Clinical features of patients infected with 2019 novel coronavirus in Wuhan, China, Lancet 395 (2020) (2019) 497–506.

[6] Centers for Disease Control and Prevention, Situation Summary COVID-19, 2020. Retrieved March 23, 2020 (https://www.cdc.gov/coronavirus/2019-nCoV/index.html).

[7] B. Shayak, M.M. Sharma, M. Gaur, & A.K. Mishra. Impact of reproduction number on multiwave spreading dynamics of COVID-19 with temporary immunity: a mathematical model, International Journal of Infectious Diseases (2021). Preprint at doi: 10.1016/j.ijid.2021.01.018.

[8] S.K. Law, A.W.N. Leung, C. Xu, Is reinfection possible after recovery from COVID-19?, Hong Kong Medical Journal 26 (2020) 264–265.

[9] P. Selhorst, S.V. Ierssel, J. Michiels, J. Mariën, K. Bartholomeeusen, E. Dirinck, S. Vandamme, H. Jansens,& K. K. Ariën.Symptomatic SARS-CoV-2 reinfection of a health care worker in a Belgian nosocomial outbreak despite primary neutralizing antibody response, Clinical Infectious Diseases, (2021). Preprint at doi.org/10.1093/cid/ciaa1850

[10] M. Galanti, J. Shaman, Direct Observation of Repeated Infections with Endemic Coronaviruses, J. Infect. Dis. 3 (2020) 409–415.

[11] H. Ledford, Coronavirus Re-infections: Three Questions Scientists Are Asking, Nature Research Journals 7824 (2020) 168–169.

[12] C. Giannitsarou, S. Kissler, F. Toxvaerd, Waning Immunity and the Second Wave: Some Projections for SARS-CoV-2, CEPR Centre for Economic Policy Research (2020).

[13] S. Kumar, R. Kumar, C. Cattani, B. Samet, Chaotic behaviour of fractional predator-prey dynamical system, Chaos, Solitons & Fractals 135 (2020) 109811.

[14] S. Kumar, S. Ghosh, B. Samet, E.F.D. Goufo, An analysis for heat equations arises in diffusion process using new Yang-Abdel-Aty-Cattani fractional operator, Mathematical Methods in the Applied Sciences (2020) 1–19.

[15] S. Kumar, R. Kumar, R.P. Agarwal, B. Samet, A study of fractional Lotka-Volterra population model using Haar wavelet and Adams-Bashforth-Moulton methods, Mathematical Methods in the Applied Sciences (2020) 1–15.

[16] S. Kumar, A. Kumar, B. Samet, H. Dutta, A study on fractional host-parasitoid population dynamical model to describe insect species, Numerical Methods for Partial Differential Equations (2020) 1–20.

[17] N. Anggriani, H. Tasman, M.Z. Ndii, A.K. Supriatna, E. Soewono, E. Siregar, The effect of reinfection with the same serotype on dengue transmission dynamics, Appl. Math. Comput. 349 (2019) 62–80.

[18] M.Z. Ndii, Z. Amarti, E.D. Wiraningsih, A.K. Supriatna, Rabies epidemic model with uncertainty in parameters: crisp and fuzzy approaches, IOP Conference Series: Materials Science and Engineering 332 (2018) 012031.

[19] S. Kumar, A. Kumar, B. Samet, J.F. Gmez-Aguilar,& M.S. Osman, A chaos study of tumor and effector cells in fractional tumor-immune model for cancer treatment, Chaos, Solitons & Fractals, 141 (2020), 110321.

[20] B. Ghanbari, S. Kumar, R. Kumar, A study of behaviour for immune and tumor cells in immunogenetic tumour model with non-singular fractional derivative, Chaos, Solitons & Fractals 133 (2020) 109619.

[21] M.Z. Ndii, A.K. Supriatna, Stochastic mathematical models in epidemiology, Information 20 (2017) 6185–6196.
[22] H. Alrabaiah, A. Mo, M.H. Safi, B. DarAssi, S. Al-Hdaibat, M. A. Ullah, S.A.A.Sh.ah. Khan, Optimal control analysis of hepatitis B virus with treatment and vaccination, Results in Physics 19 (2020) 103599.
[23] M.A.A. Oud, A. Ali, H. Alrabaiah, S. Ullah, M.A. Khan, S. Islam, A fractional order mathematical model forCOVID-19 dynamics with quarantine, isolation, and environmental viral load, Advances in Difference Equations 106 (2021) 1–19.
[24] Z. Liu, P. Magal, O. Seydi, & G. Webb., Predicting the Cumulative Number of Cases for the COVID-19 Epidemic in China from Early Data. Preprint at doi: 10.20944/preprints202002.0365.v1 (2020a).
[25] Z. Liu, P. Magal, O. Seydi, & G. Webb., Understanding Unreported Cases in the COVID-19 Epidemic Outbreak in Wuhan, China, and the Importance of Major Public Health Interventions, Biology 9(2020b).
[26] M. Pierre, G. Webb, The Parameter Identification Problem for SIR Epidemic Models: Identifying Unreported Cases, J. Math. Biol. 77 (2018).
[27] K. Biswas, A. Khaleque, & P. Sen, COVID-19 spread: Reproduction of data and prediction using a SIR model on Euclidean network, pp. 4–7, 2020, [Online]. Available: http://arxiv.org/abs/2003.07063.
[28] K. Biswas & P. Sen, Space-time dependence of corona virus (COVID-19) outbreak, no. 1, pp. 5-7, 2020, [Online]. Available: https://arxiv.org/abs/2003.03149.
[29] M.A. Khan, A. Atangana, Modeling the dynamics of novel coronavirus(2019-nCov) with fractional derivative, Alexandria Engineering Journal 59 (2020) 2379–2389.
[30] M.A. Khan, A. Atangana, E. Alzahrani, The dynamics of COVID-19 with quarantined and isolation, Advances in Difference Equations 1 (2020) 1–22.
[31] M.S. Alqarni, M. Alghamdi, T. Muhammad, A.S. Alshomrani, M.A. Khan, Mathematical modeling for novel coronavirus (COVID-19) and control, Numerical Methods for Partial Differential Equations (2020).
[32] Y. Chu, A. Ali, M.A. Khan, S. Islam, S. Ullah, Dynamics of fractional order COVID-19 model with a case study of Saudi Arabia, Results in Physics 21 (2021) 103787.
[33] S. Kumar, R. Kumar, S. Momani,& Samir Hadid, A study on fractional COVID-19 disease model by using Hermite wavelets, Mathematical Methods in the Applied Sciences, (2021), 1-17.
[34] M.A. Khan, S. Ullah, S. Kumar, A robust study on 2019-nCOV outbreaks through non-singular derivative, The European Physical Journal Plus 136 (2021) 1–20.
[35] K.M. Safare, V.S. Betageri, D.G. Prakasha, P. Veeresha, S. Kumar, A mathematical analysis of ongoing outbreak COVID-19 in India through nonsingular derivative, Numerical Methods for Partial Differential Equations 37 (2021) 1282–1298.
[36] S. Kumar, R.P. Chauhan, S. Momani, & Samir Hadid, Numerical investigations on COVID-19 modelthrough singular and non-singularfractional operators, Numerical Methods for Partial Differential Equations (2020) 1–27.
[37] Q. Lin, S. Zhao, G. Daozhou, Y. Lou, S. Yang, et al, A conceptual model for the coronavirus disease 2019 (COVID-19) outbreak in Wuhan, China with individual reaction and governmental action, International Journal of Infectious Diseases. 93 (2020) (2019) 211–216.
[38] B. Ivorra, M.R. Ferrandez, M.V. Perez, A.M. Ramos, Mathematical modeling of the spread of the coronavirus disease 2019 (COVID-19) taking into account the undetected infections. The case of China, Communications in Nonlinear Science and Numerical Simulation. 88 (2020).
[39] B. Tang, F. Xia, S. Tang, N.L. Bragazzi, Q. Li, et al, The effectiveness of quarantine and isolation determine the trend of the COVID-19 epidemic in the final phase of the current outbreak in China, International Journal of Infectious Diseases 96 (2020) 288–293.
[40] J.P. Arcede, R.L.C. Anan, C.Q. Mentuda, & Y. Mammer., Accounting for Symptomatic and Asymptomatic in a SEIR-type model of COVID-19. Preprint at https://arxiv.org/abs/2004.01805 (2020).
[41] M.Z. Ndii, A.R. Mage, J.J. Messakh, B.S. Djahi, Optimal vaccination strategy for dengue transmission in Kupang city, Indonesia. Heliyon 6 (2020) e05345.
[42] H. Sun, Y. Qiu, H. Yan, Y. Huang, Y. Zhu, et al., Tracking and Predicting COVID-19 Epidemic in China Mainland. Preprint at https://www.medrxiv.org/content/10.1101/2020.02.17.20024257v1 (2020).
[43] S. Ullah, M.A. Khan, Modeling the impact of non-pharmaceutical interventions on the dynamics of novel coronavirus with optimal control analysis with a case study, Chaos, Solitons & Fractals 139 (2020) 110075.
[44] N. Anggriani, A.K. Supriatna, E. Soewono, A Critical Protection Level Derived from Dengue Infection Mathematical Model Considering Asymptomatic and Symptomatic Classes, Journal of Physics Conference Series. 423 (2013) 1–10.
[45] V. Kontis, J.E. Bennett, T. Rashid, R.M. Parks, J. Pearson-Stuttard, M. Guillot, P. Asaria, B. Zhou, M. Battaglini, G. Corsetti, M. McKee, M. Di Cesare, C.D. Mathers, M. Ezzati, Magnitude, demographics and dynamics of the effect of the first wave of the COVID-19 pandemic on all-cause mortality in 21 industrialized countries, Nat. Med. 26 (2020) 1919–1928.
[46] O. Diekmann, J. Heesterbeek, Mathematical Epidemiology of Infectious Diseases, Wiley Series in Mathematical and Computational Biology (2000).
[47] C. Chavez, C., Z. Feng, W. Huang., On the computation of R0 and its role in global stability. In: Math ApproachesEmerg Reemerg Infect Dis Intro. IMA, 125 (2002), 229-250.
[48] J.J. Tewa, J.L. Dimi, S. Bowong, Lyapunov functions for a dengue disease transmission model, Chaos, Solitons, & Fractals 39 (2009) 936–941.
[49] J.P. LaSalle, The stability of dynamical systems, SIAM, Philadelphia, 1976.
[50] S. Marino, I.B. Hogue, C.J. Ray, D.E. Kirschner, A methodology for performing global uncertainty and sensitivity analysis in systems biology, J. Theor. Biol. 254 (2008) 178–198.
[51] A.M. Islam, A comparative study on numerical solutions of initial value problems (IVP) for ordinary differential equations (ODE) with Euler and Runge Kutta Methods, American Journal of Computational and Applied Mathematics 5 (2015) 393–404.
[52] A.J. Kucharski, T.W. Russell, C. Diamond, Y. Liu, J. Edmunds, S. Funk, R.M. Eggo, F. Sun, M. Jit, J.D. Munday, N. Davies, A. Gimma, K. van Zandvoort, H. Gibbs, J. Hellewell, C.I. Jarvis, S. Clifford, B.J. Quilty, N.I. Bosse, S. Abbott, P. Klepac, S. Flasche, Early dynamics of transmission and control of COVID-19: a mathematical modelling study, Lancet. Infect. Dis 20 (2020) 553–558.
[53] W.J. Guan, Z.Y. Ni, Y. Hu, W.H. Liang, C.Q. Ou, J.X. He, et al, Clinical Characteristics of Coronavirus Disease 2019 in China, New Engl. J. Med. 382 (2020) (2019) 1708–1720.
[54] D. Aldila, S.H.A. Khoshnaw, E. Safitri, Y.R. Anwar, A.R.Q. Bakry, B.M. Samiadji, D.A. Anugerah, M.F. Farhan GH, I.D. Ayulani, S.N. Salim, A mathematical study on the spread of COVID-19 considering social distancing and rapid assessment: The case of Jakarta, Indonesia, Chaos, Solitons and Fractals, 139 (2020), 110042.